ABSTRACT

JUNG, YONG. Transport of Emulsified Edible Oil in a 3-Dimensional Sandbox: Experimental and Modeling Results. (Under the direction of Robert C. Borden)

Injection of edible oils into the subsurface can provide an effective, low-cost alternative for stimulating anaerobic bioremediation processes. However concerns have been raised about the effects of oil buoyancy and variations in aquifer permeability on the final distribution of oil in the subsurface. 3-D sandbox experiments (1.2 m x 0.98 m x 0.98 m) were conducted to study the distribution of edible oil emulsions. In the first homogeneous experiment, the sandbox was packed with fine clayey sand (D_{50} = 0.38 mm, 6.9 % passing #200 sieve). In the second heterogeneous experiment, the sandbox was packed in three layers with the fine clayey sand amended with varying amounts of kaolinite (2.5%, 0%, and 5%). A continuously screened injection well was located in one corner of the sandbox. No flow boundaries were located on the two sides directly adjoining the well and constant head boundaries were located on the two sides opposite from the well to simulate ¼ of the flow-field surrounding an injection well. A fine emulsion was first injected through the well followed by chase water to distribute the emulsion throughout the sandbox. This approach was very effective in distributing the oil throughout the sandbox and resulted in a reasonably uniform volatile solids distribution in the top, middle and bottom layers, measured 5 ~ 7 weeks after the completion of emulsion injection.

The numerical model RT3D with sorption represented by a mass-transfer limited, Langmuir isotherm was used to simulate emulsion transport and retention in the 3-D sandbox. All model parameters, with the exception of the mass transfer rate, were measured independently. Simulations results were in close agreement with observed values for both the homogeneous and heterogeneous injection tests demonstrating that this approach can be used to describe the transport and distribution of emulsified oil under representative aquifer conditions.

Transport of Emulsified Edible Oil in a 3-Dimensional Sandbox: Experimental and Modeling Results

by

YONG JUNG

A thesis submitted to the Graduate Faculty of
North Carolina State University
in partial fulfillment of the
requirements for the Degree of
Master of Science

DEPARTMENT OF CIVIL, CONSTRUCTION AND ENVIRONMENTAL ENGINEERING

Raleigh

2003

North Carolina State University

BIOGRAPHY

Yong Jung was born on January 26, 1973, in Kwangju, South Korea. He was raised in Kwangju city until his college year. In the spring of 1991, he attended Chosun University in the major of civil engineering. After his college, he worked for the division of civil engineering of the 91st Airbase Construction Group in the Korean Air force as an officer for four years. In the air force, he supervised two different construction sites for anti aircraft artillery SQ, and designed several new-year designing projects. In 1999, he started to work at Daewoo engineering for airport designs in Korea. Kimhae international additional development design and Chonju international airport are one of his major works in the Daewoo engineering.

He began his graduate education at North Carolina State University in 2001 in fall semester for environmental engineering about anaerobic bioremediation methods for ground water. He was a research assistant for four semesters under Robert C. Borden.

ACKNOWLEDGEMENTS

The author sincerely gives this thesis to the Lord.

The author would like to appreciate Dr. Robert C. Borden for his technical and emotional guidance, support, and his patience throughout whole author's graduate school. The author has respect for his humility and passion for his researches.

Specially thanks to Dr. Ranji Ranjithan and Dr. Mohammed Gabr for their time and efforts for the examination.

The author would like to thank to Kapo Coulibaly, Nick Lindow, Cam Long, and Ximena Rodriguez for their help and encouragement and NC State Korean Civil Engineering Association members.

The author will remember the time with good friends, Julie Larsen, ZhengZheng Hu, Doug Christie, Yeon Noh, Luki Mahanani, and other many friends. In addition, the author specially thanks for the lovely support from David & Katherine Kesterson, Bill & Laura Miller, Leon Jr. & Carolyn Cheek, and Claire Drehmel.

The author is truly indebted to his lovely parent (Dangchae Jung, Yanglim Choi) and my brother, Kwon's family and sister, Hairang's family.

TABLE OF CONTENTS

List of Tables

List of Figures

1. Introduction

A variety of anaerobic bioremediation processes are being developed for the in-situ treatment of groundwater contaminants including chlorinated solvents, perchlorate (ClO_3^-), chromate (CrO_4^{-2}), nitrate (NO_3^-) and acid mine drainage (Morse et al., 1998; Hunter, 2001; Hunter, 2002; ARCADIS, 2002; ITRC, 2002). Essentially all of these processes require that the contaminant be brought in contact with a biodegradable organic substrate (Nyer, 1985; Thomas et al., 1989). This substrate serves as a carbon source for cell growth and as an electron donor for energy generation.

The most common approach for stimulating in-situ anaerobic biodegradation is to flush a dissolved substrate through the contaminated zone using a series of injection and production wells. This approach has been very effective at some sites (Ellis et al., 2000; Martin et al., 2001; Major et al., 2002). However continuously feeding a soluble, easily biodegradable substrate can be expensive. There is a significant initial capital cost associated with installation of the required tanks, pumps, mixers, injection and pumping wells, and related process controls. In addition, operation and maintenance (O&M) costs can be high because of problems associated clogging of pumps, piping, and mixers and the labor for monitoring and process control. An alternative approach employed at some sites has been to distribute a 'slow-release' organic substrate to support anaerobic biodegradation of the target contaminants. A variety of slow-release substrates have been proposed including chitin (Harkness, 2003; Martin et al., 2002), Hydrogen Release Compound (Koenigsberg, 2000; Wu 1999), and emulsified edible oils (Zenker et al., 2000; Lee et al., 2001; Wiedemeier et al., 2001).

We are working to develop an effective, low cost process for stimulating in-situ anaerobic bioremediation processes using food-grade edible oils. In this process, an oil-in-water emulsion is prepared using edible oil, food-grade surfactants and an appropriate high-

shear mixer. This emulsion is then injected into the sediment followed by chase water to distribute and immobilize the oil. The immobilized oil then serves as a slow-release carbon source to support anaerobic biodegradation of the problem contaminants. Capital costs for stimulating anaerobic bioremediation processes using emulsified oils are expected to be much lower than competing technologies since most of the injection equipment can be reused at multiple sites. Long-term operation and maintenance costs should also be lower since much less frequent substrate addition would be required (Harkness, 2000).

Coulibaly and Borden (2003) have presented laboratory results showing that emulsions prepared using food-grade soybean oil can be effectively distributed in sands and clayey sands with only modest reductions in aquifer permeability (0 to 40% reduction in K). The key to effective oil transport appears to be in preparing an emulsion with small, uniformly sized oil droplets. When the oil droplets are smaller than the pore diameters, the droplets can be transported significant distances through porous media (Soo and Radke, 1986). Oil retention and associated reductions in permeability increases with sediment clay content and with the ratio of droplet size to pore size (Coulibaly and Borden, 2003). Emulsion droplet transport in sandy sediments can be described using standard solute transport models modified to simulate oil retention using a rate-limited Langmuir isotherm (Coulibaly et al., submitted).

While the available laboratory and field data indicate that emulsions can be effectively distributed in typical aquifer materials, some questions still remain.

- Edible oils are less dense than water so there is potential for buoyancy effects that could result in poor oil distribution in deeper portions of the aquifer where contaminant concentrations may be high.
- In-situ treatments are often complicated to implement because difficulties associated with distributing treatment agents throughout heterogeneous aquifers.

In this work, radial flow injection experiments were conducted in a 3-dimensional (3-D) laboratory sandbox to study the oil injection process under representative conditions and to identify injection approaches that are less sensitive to aquifer heterogeneity. Emulsion injection tests were conducted for two aquifer conditions: (1) homogenous sand; and (2) a moderate permeability sand layer between two lower permeability clayey sand layers. These experimental results were then used to validate the numerical model RT3D (Clement, 1997) for simulating emulsion transport where emulsion retention by the sediment is described by a rate-limited Langmuir isotherm (Coulibaly et al., submitted).

2. Materials and methods

The experimental setup was designed to simulate one quarter of the flow-field adjoining an emulsion injection point. A plan view of the sandbox and injection well is shown in Figure 1. The inside dimensions of the sandbox are 0.98 m wide x 0.98 m deep x 1.2 m high. A double layer of geonet drainage material and single layer of non-woven geotexile fabric are installed along the back and right boundaries. These drainage layers are connected by several different ports to a single reservoir that maintained the back and right sides as constant head boundaries. A 2.5 cm diameter x 100 cm long slotted well screen (#20 slot) was located in the front left corner of the sandbox and connected to a constant head reservoir. With the front and left sides of the tank acting as no-flow boundaries, this setup reasonably represents one quarter of the flow field surrounding an injection point. The 1.0 m injection radius in the laboratory experiment is at a scale comparable to field conditions.

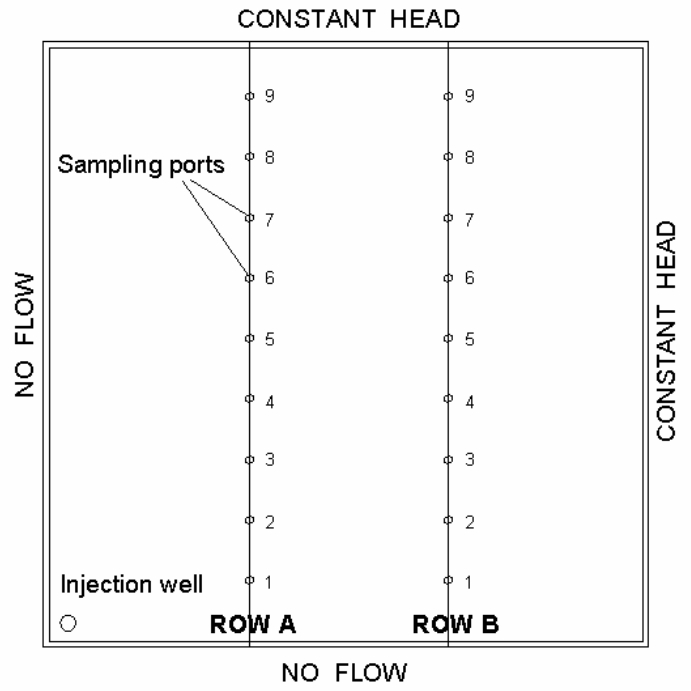

Figure 1 Plan view of the 3-D sandbox showing the sample/manometer tube locations.

The oil-in-water emulsions used in these experiments were prepared by blending 87.4 % tap water, 11 % soybean oil, and 1.6 % premixed surfactant (38% polysorbate 80, 56% glycerol monooleate and 6% water). The emulsion used in the first homogeneous test was prepared in a standard high-speed lab blender (Waring Commercial Blender) while the emulsion used in the second heterogeneous test was prepared in a high pressure dairy homogenizer (Gaulins two stage 300 GCI at 1000 psi). The droplet size distribution for each emulsion was measured visually with a Nikon™ microscope equipped with a Sensys™ calibrated camera and Metamorph™ software at a 400x magnification. In the homogeneous test, the median droplet diameter was 1.2 μm while the median diameter in the heterogeneous tests was 0.7 μm. The cumulative oil volume versus droplet diameter for the emulsions used in the homogeneous and heterogeneous injection tests are presented in Figure 2. Photomicrographs of the emulsions used in each test are presented in Appendices A1 and B1.

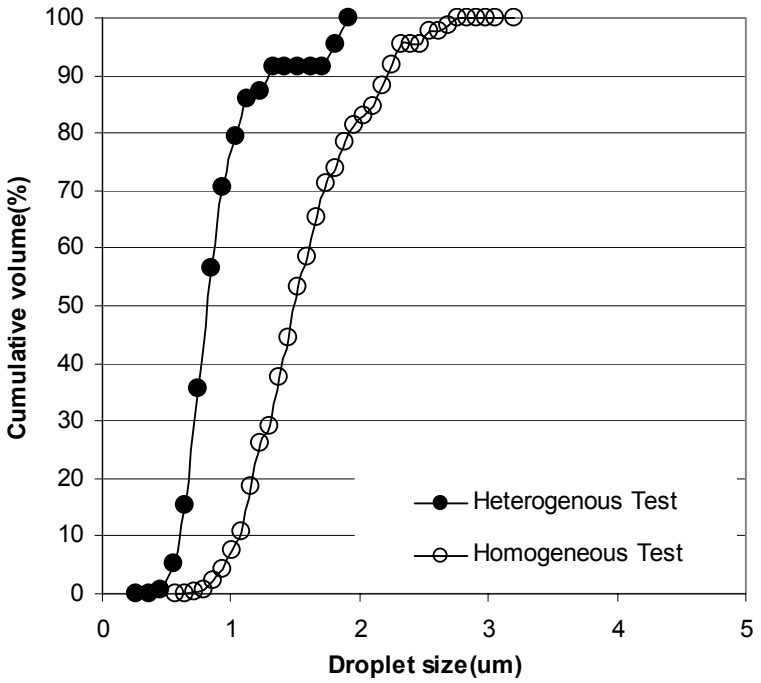

Figure 2 Cumulative droplet volume distributions for homogeneous and heterogeneous injection tests.

Liquid samples were collected throughout both tests to monitor emulsion breakthrough with time. Soil cores were collected 5 weeks after completion of the homogeneous and 7 weeks after completion of heterogeneous test to measure the final oil distribution. Liquid and sediment samples were analyzed for volatile solids (VS) by weight loss on ignition for 1 hour at 550 ºC.

2.1. Homogeneous Injection Test

For the homogeneous test, a 5 cm thick bentonite layer was placed in the bottom of the tank followed by 110 cm of 'field sand' (fine clayey sand, D_{50} = 0.38 mm, D_{10} = 0.09 mm, D_{60}/D_{40} = 3.9, 6.9 % passing #200 sieve). A second 10 cm thick bentonite layer was placed above the sand to form a confining layer allowing emulsion injection under a slight pressure (~ 18 cm of water). During sand placement, 10 – 20 cm of water was maintained above the

sand surface. Approximately 10 L of sand was placed at a time followed by gentle mixing of the sand surface and compaction to remove entrapped air. On a macroscopic scale, this resulted in reasonably uniform packing with little entrapped air. However visual inspection of the sand through the clear acrylic plastic showed some small-scale segregation of sediments where some thin layers appeared to have more clay than others. Two rows (shown as A and B on Figure 1) of 2 mm ID stainless steel tubes with nylon screens were installed at 25 cm, 50 cm, and 75 cm from the top of the sand layer for sample collection and to measure changing water levels via a manometer board. Additional details on the tank construction and sampling tube locations are presented in Appendix A2. Based on the weight of added sand, the final porosity (n) and bulk density (ρ_B) were 0.36 and 1.77 g/cm^3, respectively. Hydrodynamic parameters were estimated using results from a non-reactive tracer test where 60 L (~0.2 PV) of a 200 mg/L NaBr solution was injected followed by 450 L (~1.5 PV) of tap water over a 5 day period. During the emulsion test, 30 L (~ 0.1 PV) of oil-in-water emulsion were injected followed by 450 L of tap water (~1.5 PV) to distribute and immobilize the oil.

2.2. Heterogeneous Injection Test

In the heterogeneous test, a 5 cm bentonite layer was installed on the bottom of the tank, followed by 23 cm of field sand amended with 5% kaolinite (n = 0.26, ρ_B = 1.96 g/cm^3), 48 cm of field sand (n = 0.22, ρ_B = 2.07 g/cm^3), 29 cm of field sand amended with 2.5% kaolinite (n = 0.30, ρ_B = 1.84 g/cm^3) and 20 cm of bentonite to form a confining layer. The field sand – kaolinite mixtures were prepared by blending known weights of field sand and kaolinite (Standard Industrial Mineral Inc. Bishop, CA) in concrete mixer for ~ 15 minutes per batch. The stainless steel sampling tubes were screened at 90 cm, 50 cm, and 25 cm from the bottom of the bentonite layer. Additional details on the tank construction and sampling

tube locations are presented in Appendix B2. In the heterogeneous test, the non-reactive tracer was injected as part of the emulsion. Prior to injection, tap water was flushed through the tank for 2 weeks to establish steady-state conditions. The emulsion injection test consisted of injecting 120 L (~0.5 PV) of emulsion amended with 1000 mg/l NaCl followed by 1000 L (~5.0 PV) of tap water.

3. Emulsion Injection Test Results

3. 1. Homogeneous Injection Test

Prior to the start of emulsion injection, a non-reactive tracer test was run and the spatial variation of head with distance was determined to collect data required for calibration of a groundwater flow and solute transport model (described in Section 4 and Appendix A3). During emulsion injection, the flowrate dropped to 0.06 m^3 /d from a pre-injection value of 0.13 m^3 /d (std. dev. = 0.01). Shortly after the start of the post-emulsion water flush, the flowrate recovered to 0.10 m^3 /d and then remained relatively constant for the remainder of the test (ave. flow = 0.11 m^3 /d, std. dev. = 0.01). Water levels in the injection well and constant head boundaries were held constant throughout the test, so the decline in flowrate during emulsion injection indicates a temporary reduction in the effective hydraulic conductivity. Most of this reduction appears to be due to the somewhat higher viscosity (μ = 1.44 centipoises) and lower density (ρ = 0.99 g/cm^3) of the emulsion compared to that of water (μ = 0.95 centipoises, ρ = 1 g/cm^3). The recovery in injection flowrate during the post-emulsion water flush indicates that there was no significant, long-term permeability loss associated with the emulsion injection. These results are consistent with prior work by Coulibaly and Borden (2003) who showed that flushing 3 pore volumes (PV) of a similar emulsion (median droplet diameter = 1.2 μm) followed by 7 PV of water through the same field sand resulted in only 3% reduction in hydraulic conductivity.

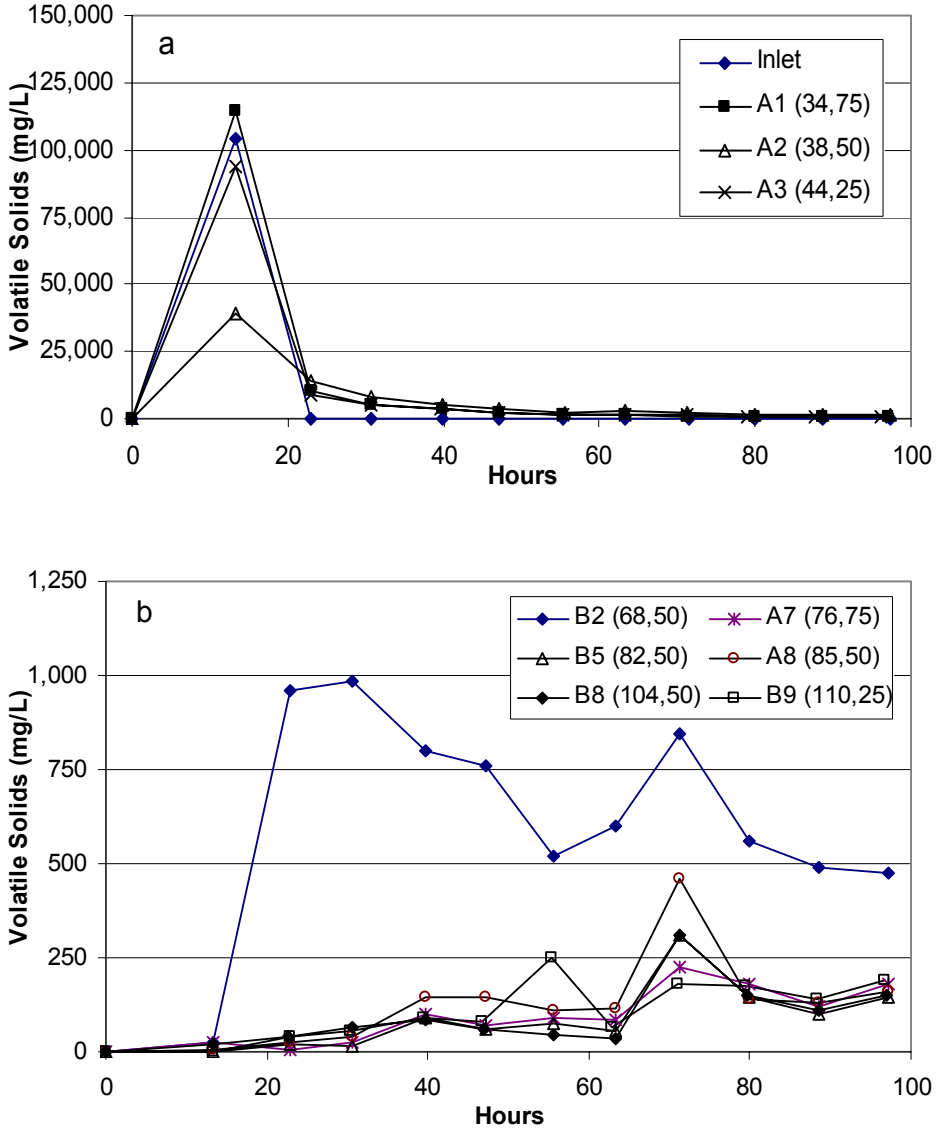

Figure 3 Volatile solids concentration versus time in the injection feed and monitoring points. Values in parentheses indicate radial distance from the injection well (cm) and depth from the top of sand (cm).

Figure 3 shows the variation in emulsion concentration versus time in monitoring points close to the injection well (Figure 3a) and more distant from the injection well (Figure 3b). The maximum concentrations observed in the closest monitoring points were 110%, 37% and 90% of the injection concentration indicating essentially complete emulsion

breakthrough at up to 44 cm from the injection well. In the more distant sampling points, emulsion breakthrough was more limited and occurred later in the test as the chase water distributed emulsion throughout the sandbox. In sampling points over 70 cm from the injection well, emulsion concentrations never exceeded 0.5% of the injected concentration. This is in contrast to the non-reactive tracer test results which showed 50% to 100% breakthrough at the same locations and indicates that most of the emulsion was captured by the soil matrix.

Five weeks after the end of the emulsion injection test, sediment cores were collected from 9 locations to determine the spatial distribution of residual emulsion in the sediment. During this post-injection period, there was no flow through the tank to evaluate the potential for oil droplets to float upward due to buoyancy effects. Figure 4 shows the sediment volatile solids (VS) concentration (mg/g) after correcting for the sediment VS prior to injection (5.39 mg/g). The VS results show that emulsion was effectively distributed throughout the tank. However there was a statistically significant trend in VS concentration with radial distance at each depth with slightly higher concentrations in samples collected closer to the injection well. There was no significant difference in sediment VS concentrations between the three sampling zones indicating that buoyancy effects were not significant.

Approximately 67.5% (95% confidence limits = ± 24 %) of the added emulsion was retained by the sediment based on the average VS in the sandbox (mean = 1.85, std. dev. = 1.66, n = 27) and the amount of sediment in the sandbox. Sampling from one of several discharge ports on the constant head boundaries indicated that 2.5% of the emulsion was released in the sandbox effluent with up to 30% of the emulsion unaccounted. However visual observations indicated considerable variability in emulsion concentration between the different constant head discharge ports, suggesting that more emulsion may have been released in the sandbox discharge than the sampling results indicate.

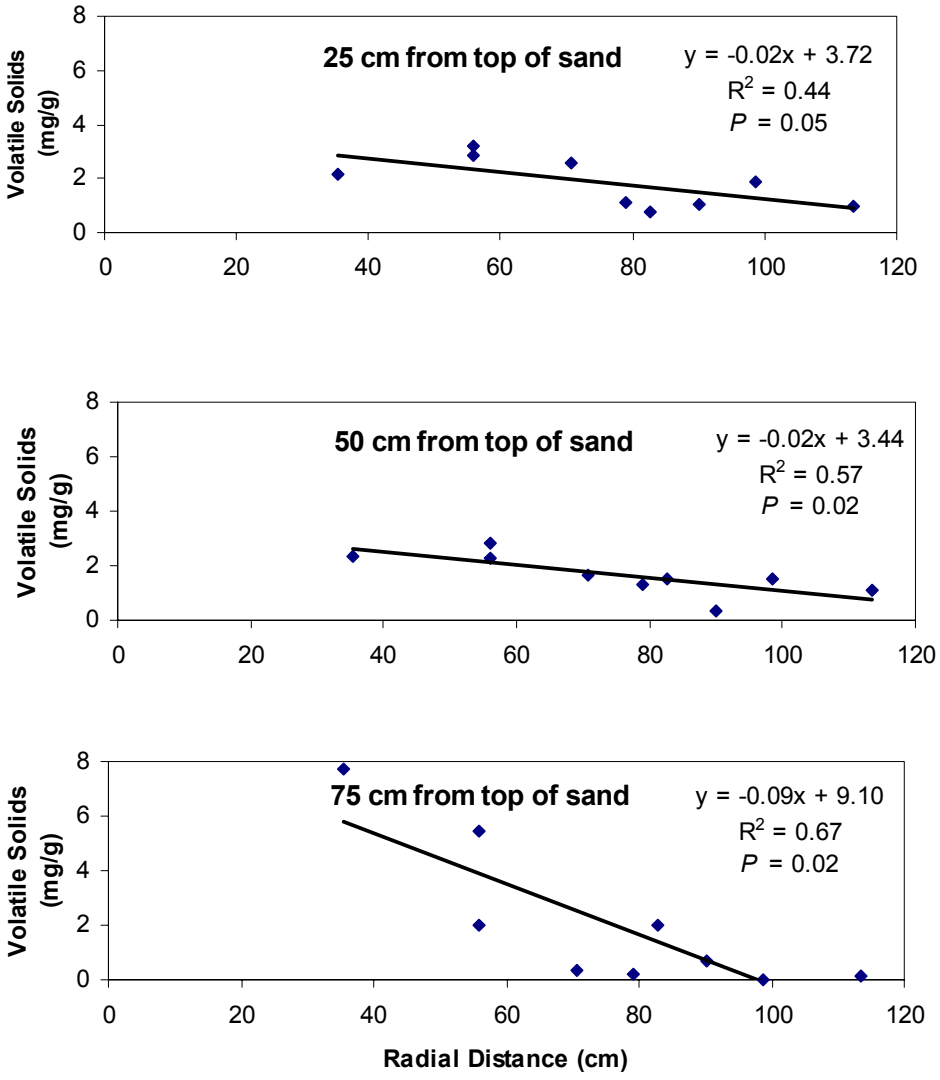

Figure 4 Volatile solids concentration in sediment samples collected 5 weeks after the end of homogeneous injection test.

3.2. Heterogeneous Injection Test

Prior to the start of emulsion injection, tap water was run through the tank at a flowrate of 0.6 m^3/d for several weeks to establish steady-state conditions. The spatial variation of head with distance was determined for groundwater model calibration (described in Section 4 and Appendix B3). The emulsion injection test consisted of injecting 120 L

(~0.5 PV) of emulsion amended with 1000 mg/l NaCl followed by 1000 L (~5.0 PV) of tap water.

During the emulsion injection portion of the test (0 to 10 hr), the flowrate dropped from a pre-injection value of 0.6 m^3/d (std. dev. = 0.03) to 0.2 – 0.4 m^3/d (Fig. 5A). When the injection solution was switched back to tap water at 10 hr, the injection flowrate recovered to near pre-injection values and then declined toward the end of the test. Towards the end of the heterogeneous test, we also observed an increase in head in monitoring points directly adjoining the constant head boundaries suggesting that the non-woven fabric forming the constant head boundary was being gradually clogged with fine sediment. We hypothesize that this clogging was due to mobilization of the added kaolinite by the surfactants used to form the emulsion. In prior studies (Coulibaly and Borden, 2003), we observed kaolinite mobilization by emulsion injection in field sand amended with varying amounts of kaolinite. The variation in transmissivity with time was evaluated by fitting injection flowrate and hydraulic head results from six different monitoring points to the steady-state Theim equation (Fig. 5B). These results show an apparent reduction in hydraulic conductivity immediately after emulsion injection and then an immediate recovery to pre-injection values. Towards the end of the heterogeneous test, there appears to be a slight increase in transmissivity, possibly due to mobilization of some fraction of the kaolinite. However the slight increase was not significant at the 95% confidence level.

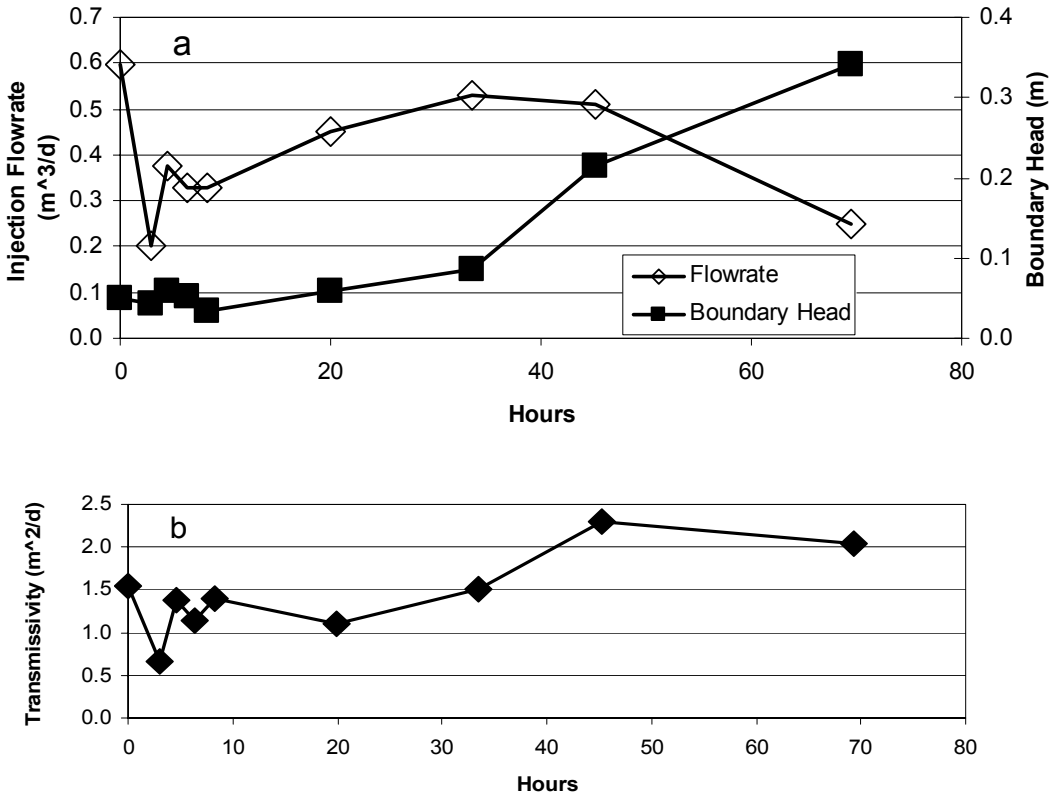

Figure 5 Variation in injection flowrate and head in monitoring point closest to constant head boundary during heterogeneous test (a). Variation in transmissivity with time (b) determined by fitting water levels in different monitoring points to steady-state Theim equation.

During the heterogeneous test, the emulsion contained a non-reactive tracer (1000 mg/L NaCl) for comparison with the emulsion breakthrough results. Figure 6 shows the breakthrough in relative concentrations of volatile solids and conductivity in sampling ports in the top, middle and bottom layers of the sandbox at different radial distances. Relative concentrations were calculated as the concentration measured at the sampling point (C) divided by concentration in the initial emulsion/tracer solution (Co). Conductivity was used as a surrogate measure of NaCl. In all the sampling points, the peak emulsion concentration was observed at the same time or slightly before the peak tracer concentration. Early colloid breakthrough has been observed in a number of previous studies (Enfield et al., 1989, Higgo

et al., 1993, Grindrod et al., 1993, 1996, Kretzschmar et al., 1995, 1998) and has generally been attributed to colloid exclusion from the smaller soil pores.

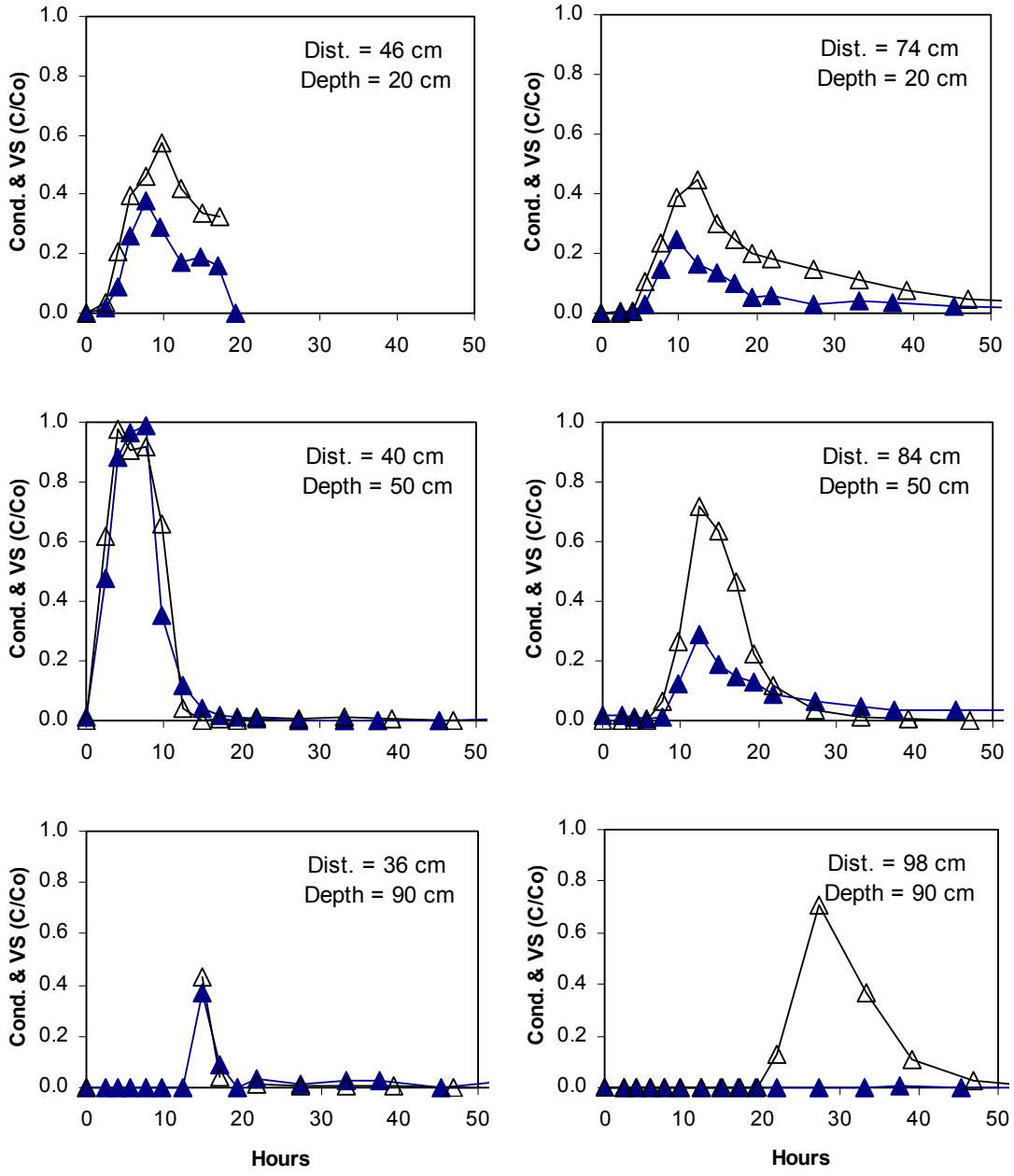

Figure 6 Variation in relative conductivity (Cond.) or volatile solids (VS) with time in selected sampling ports during heterogeneous injection test. Concentrations are plotted as measured concentration (C) divided by emulsion concentration (Co).

Figures 7a, 7b and 7c show the emulsion breakthrough with time in the upper (field sand + 2.5% clay), middle (field sand) and lower (field sand + 5% clay) layers. In the field sand layer, the maximum emulsion concentration in sampling points closest to the injection wells were close to 100% of the injection concentration, similar to results obtained during the homogeneous test. However in the heterogeneous test, high emulsion concentrations were observed further out in the field sand layer, possibly due to the greater amount of emulsion injected (0.5 PV of emulsion) and longer duration of water flushing.

In the field sand + 2.5% clay and field sand + 5% clay layers, emulsion quickly reached the wells closest to the injection well but maximum concentrations were lower than in the field sand layer and concentrations declined much more rapidly with distance from the injection point. This may be due to the higher capacity of field sand amended with clay to retain emulsion (Coulibaly and Borden, 2003).

Figures 8a, 8b and 8c shows the VS concentration of sediment samples collected at 20 cm (field sand + 2.5% clay), 50 cm (field sand) and 90 cm (field sand + 5% clay) from the top of the sandbox, 7 weeks after the completion of the emulsion injection. As in the homogeneous experiment, there was no flow through the box for this period to evaluate the effects of oil buoyancy. VS associated with the emulsion was determined by subtracting the background VS of the sediment (field sand = 3.83 mg/g, Std. dev. = 2.33; field sand + 2.5% clay = 1.59 mg/g, Std. dev. = 1.71; field sand + 5% clay = 2.07 mg/g, Std. dev. = 1.70). The sediment coring results show that emulsion was very effectively distributed throughout the field sand layer with no significant trend in VS concentration with distance. However in the field sand + 5% clay layer, VS concentrations were highest close to the injection well with lower concentrations further out. The more limited emulsion distribution in this layer is presumably due to the lower hydraulic conductivity of this layer. Results from the field sand + 2.5% clay layer were intermediate between two other layers. VS concentrations appear to

be somewhat higher near the injection well; however this trend was not significant at the 95% confidence level. As in the homogeneous test, there was no significant difference in VS in the bottom, middle and top layers indicating buoyancy effectives did not have a substantial impact on the final emulsion distribution.

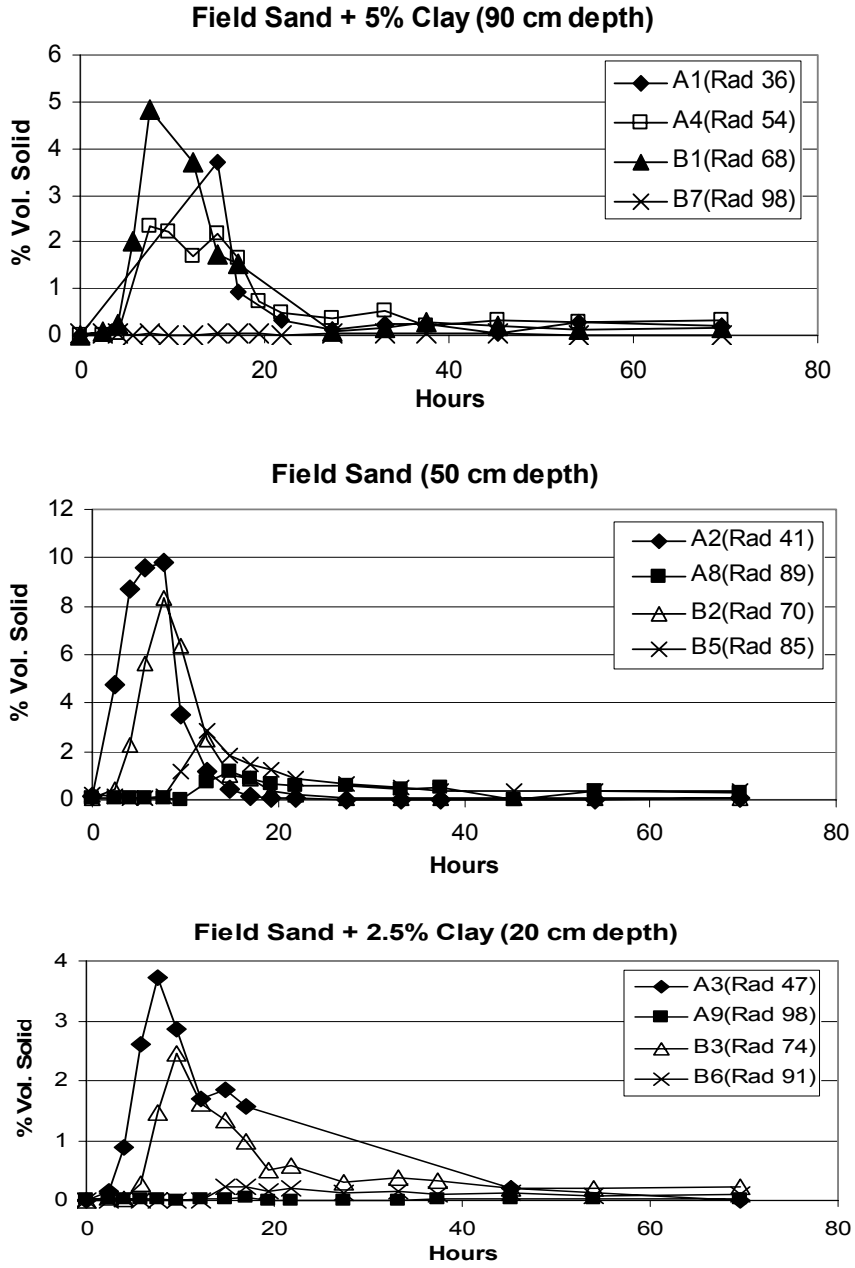

Figure 7 Volatile solids variation with time in the monitoring points during the heterogeneous test. Values in parentheses indicate radial distance from the injection well (cm).

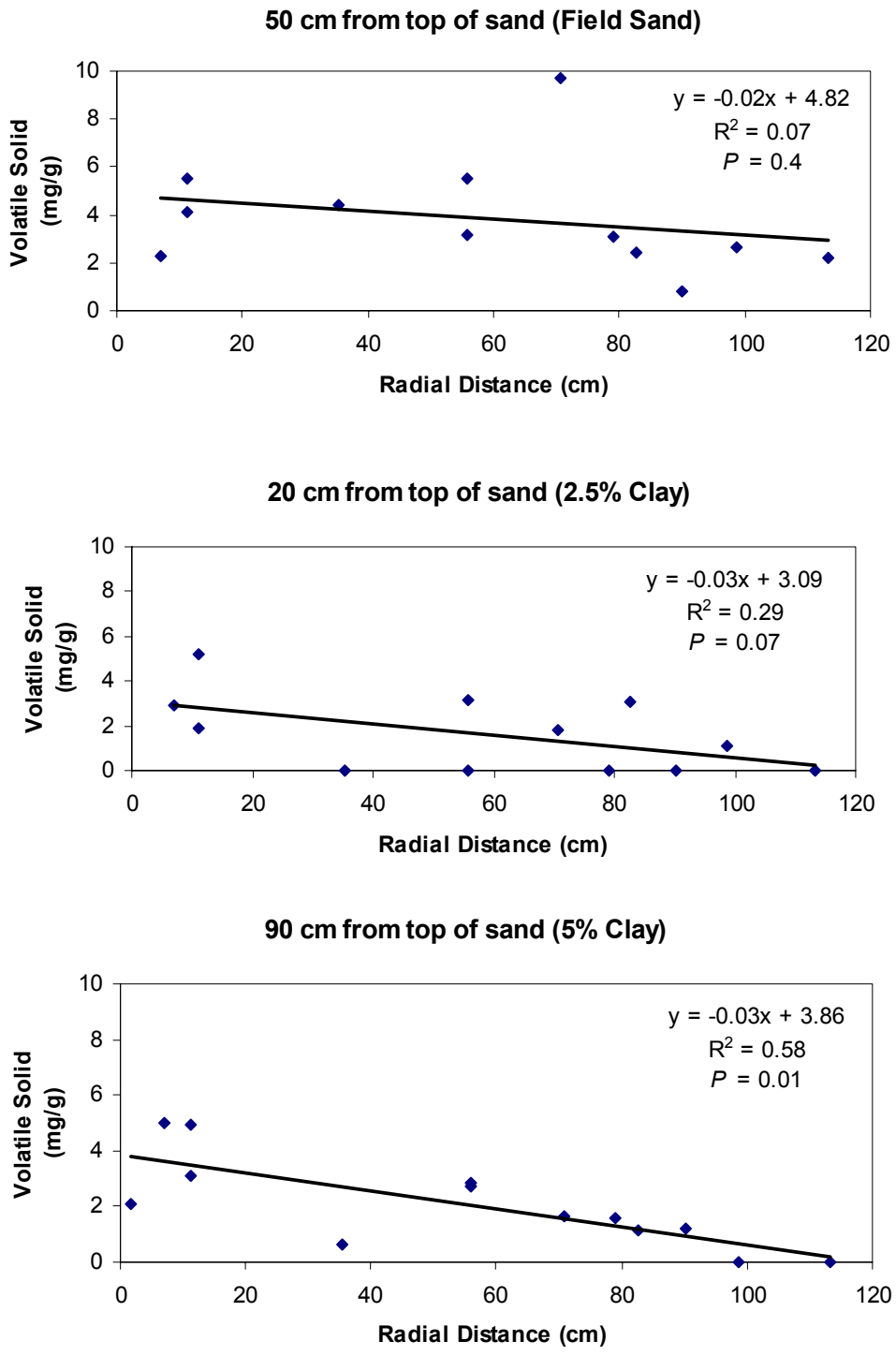

Figure 8 Volatile solids concentration in sediment samples collected 7 weeks after the end of heterogeneous test.

In the heterogeneous test, a total of 13.2 kg of VS were injected as emulsion or 11.87 mg/g of sediment. Seven weeks after the end of the injection, the average VS of the sediment was 2.51 mg/g (95% confidence limits = ± 0.67 mg/g) or 43% of the amount injected. In addition, 36.5% of the injected emulsion was observed in the sandbox effluent leaving 20.5% unaccounted. The greater amount of emulsion discharged from the sandbox in the heterogeneous test is presumably due to the much larger amount of emulsion injected and longer duration of water flushing.

4. Mathematical Modeling of Emulsion Transport and Immobilization

In previous work, Coulibaly et al. (submitted) demonstrated that transport and retention of edible oil emulsions in sandy sediments could be simulated using the standard advection-dispersion representation of mass transport modified to simulate emulsion retention as a mass-transfer limited, non-linear Langmuir isotherm:

$$\frac{\partial C}{\partial t} = \frac{\partial}{\partial x_i}\left(D_{ij} \frac{\partial C}{\partial x_j} \right) - \frac{\partial}{\partial x_i}\left(v_i C\right) - K_m (C - C^*) \qquad [1]$$

and

$$\frac{\partial S}{\partial t} = K_m \frac{\theta}{\rho} (C - C^*) \qquad [2]$$

where

$$C^* = S(K_1 K_2 - K_1 S)^{-1} \qquad [3]$$

C = liquid phase concentration (ML^{-3})

t = time (T)

x_i = distance (L)

D_{ij} = dispersion coefficient (L^2T^{-1})

v_i = pore water velocity (LT^{-1})

K_m = liquid-solid mass transfer rate (T^{-1})

ρ = bulk density (ML^{-3})

θ = porosity (dimensionless)

C* = aqueous concentration in equilibrium with the solid phase (ML^{-3})

S = solid phase concentration ($M\ M^{-1}$)

K_1 = binding constant (ML^3)

K_2 = maximum sorption capacity ($M\ M^{-1}$)

This approach was implemented within the numerical model RT3D (Clement, 1997) by developing a user defined module to simulate the change in C and S with time due to oil droplet retention by the solid phase. The user defined model was then compiled as a dynamic link library (dll) and is called by RT3D at runtime. Groundwater flow was simulated using MODFLOW (MacDonald and Harbaugh, 1988). The grid generation, data input and visualization of model results were completed using GMS 3.1 (Brigham Young University, 1999).

The sandbox was represented in plan view by a 20 x 20 grid where each cell was 5 cm x 5 cm. In the homogeneous experiments, the sandbox was simulated as a single vertical layer. In the heterogeneous experiments, the sandbox was represented by three separate layers. No flow and constant head boundary conditions were implemented where appropriate. Porosity was calculated from the sediment specific gravity and the dry weight of sediment added to each layer. For both the homogeneous and heterogeneous tests, the total transmissivity of sandbox was obtained by fitting water level monitoring results to the steady-state Theim equation. For the heterogeneous test, the transmissivity of each layer was

estimated based on the layer thickness and hydraulic conductivity measurements in standard laboratory permeameters (ASTM d 2434). Dispersivity was estimated by fitting MT3D (Zheng, 1990) to match results from non-reactive tracer tests (calibration results not shown). The Langmuir sorption parameters (K_1 and K_2) were taken from the values previously determined by Coulibaly et al. (submitted) for these materials. The initial estimates of the mass transfer rate (K_m) were also taken from Coulibaly et al. (submitted). However preliminary simulation results showed that acceptable model fits could not be obtained with the K_m values from Coulibaly et al. (submitted) and the mass transfer rate was adjusted by trial and error until a reasonably good match between the simulated and observed results was achieved. Values for the independently measured model parameters are summarized in Table 1. The initial estimates and best fit values the mass transfer rates are compared in Table 2.

Table 1 Physical and chemical parameters for homogeneous and heterogeneous injection tests.

	Homogeneous test	**Heterogeneous test**
Hydraulic Conductivity, K (m/d)	1.47	Layer 1 = 1.46
		Layer 2 = 1.50
		Layer 3 = 0.53
Porosity	0.27	Layer 1 = 0.30
		Layer 2 = 0.22
		Layer 3 = 0.26
Dispersivity (m)	0.08	0.08
Pumping rate before emulsion injection (m^3/d)	0.13	0.598
Bulk Density (kg/m^3)	1,700	Layer 1 = 1,840
		Layer 2 = 2,070
		Layer 3 = 1,960
Emulsion Injection Concentration (mg/L)	104,330	98,900
Binding Constant, K_1 (L/mg)	0.041	Layer 1 = 0.0085
		Layer 2 = 0.041
		Layer 3 = 0.0035
Maximum Sorption Capacity, K_2 (g/g)	0.005	Layer 1 = 0.007
		Layer 2 = 0.005
		Layer 3 = 0.010

Table 2 Comparison of initial parameter estimates and best fit values for mass transfer rate.

Parameter	Mass transfer rate, K_m (day^{-1})	
	Initial Estimate	Best Fit
Homogeneous test – field sand	73	1.0
Heterogeneous test – field sand	73	1.5
Heterogeneous test – field sand + 2.5% clay	360	0.7
Heterogeneous test – field sand + 5% clay	360	1.0

The variation in simulated and observed sediment VS concentrations versus radial distance is presented in Figure 9 for the homogeneous injection test and Figure 10 for the heterogeneous test. Appendix C shows the final volatile solids contour in sediment.

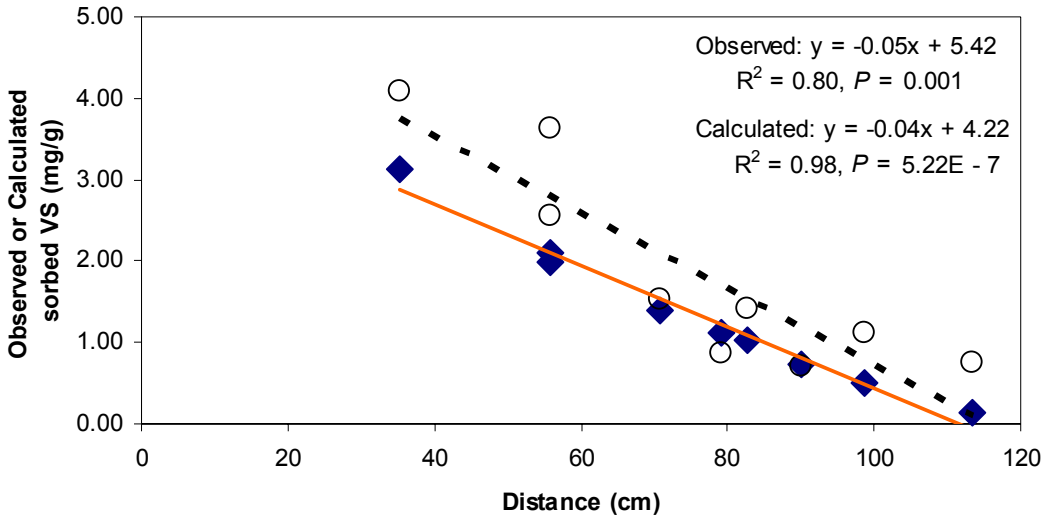

Figure 9 Variation in simulated (filled diamonds) and observed (open circles) sediment volatile solids concentration versus radial distance from the injection well for the homogeneous injection experiment. Observed concentrations are corrected for background VS.

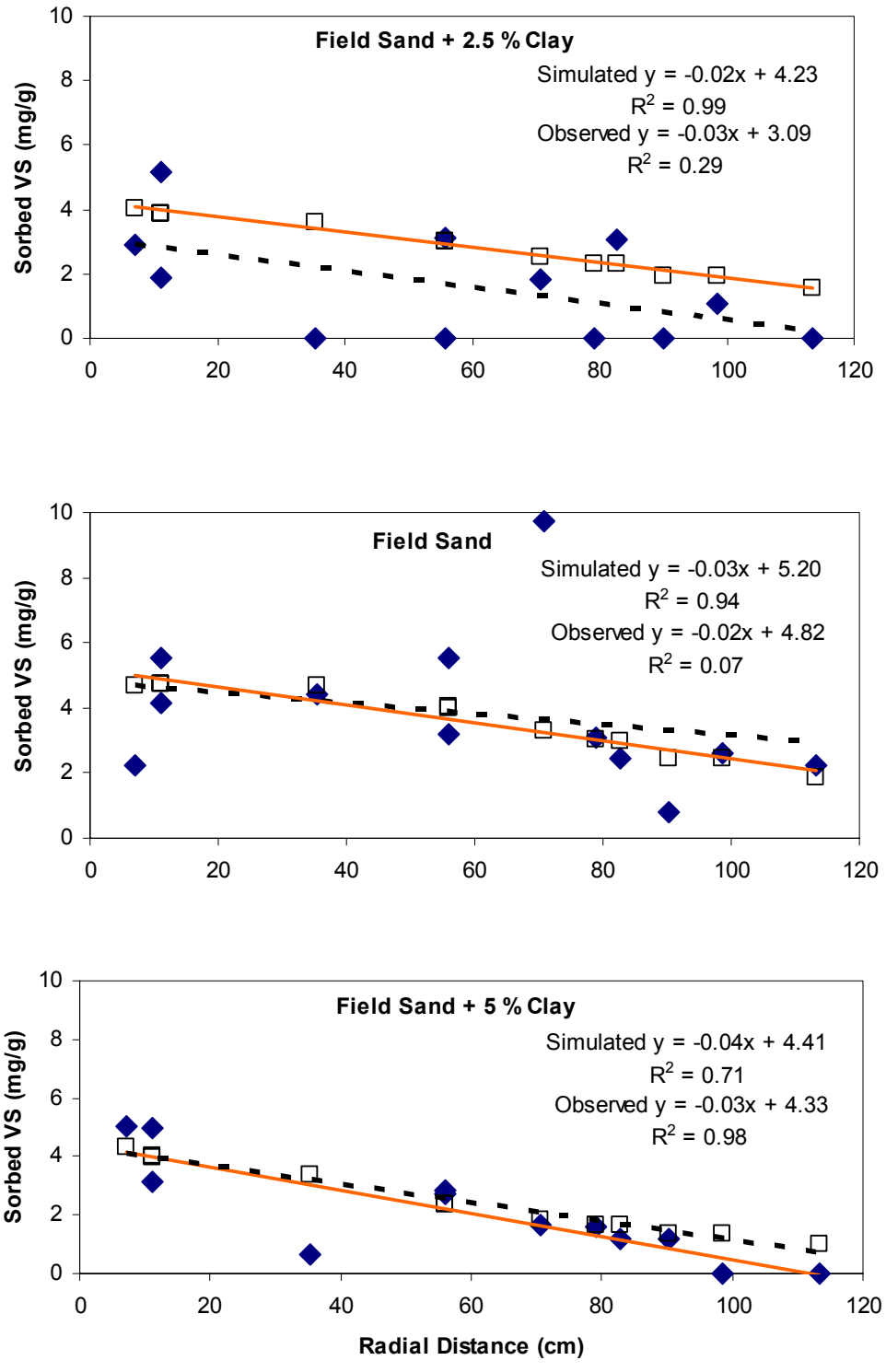

Figure 10 Variation in simulated (filled diamonds) and observed (open squares) sediment volatile solids concentration versus radial distance from the injection well for the heterogeneous injection experiment. Observed concentrations are corrected for background VS.

The model simulation results are within the experimental range of the observed concentrations and closely match the average trends for both the homogeneous and heterogeneous tests. The only location where the model fit is somewhat less than desired is for the FS + 2.5% clay layer in the heterogeneous test. In this layer, the model predicts somewhat higher sorbed VS concentrations than observed. The difference between simulated and observed VS concentrations could be due to an overestimation of the hydraulic conductivity (K) of this layer. In the model simulations, the hydraulic conductivity of the FS+2.5% clay layer was estimated to be 1.46 m/d based on a separate laboratory permeameter test. This value is only 3% less than the value used for the field sand layer. If the actual permeability of the FS+2.5% clay layer was lower than the value used in the model, the flowrate and associated emulsion transport into this layer would be lower than simulated.

Simulated versus observed concentrations for the homogeneous and heterogeneous tests are compared in Figure 11. The match between simulated and observed concentrations in sediment is remarkably good considering that all model parameters, with the exception of the mass transfer rate, were independently measured. The two order of magnitude difference between the values determined by Coulibaly et al. (submitted) and the best fit values of the mass transfer rate indicates that mass transfer rates measured in small laboratory columns cannot be used in larger scale systems (e.g. laboratory sandboxes).

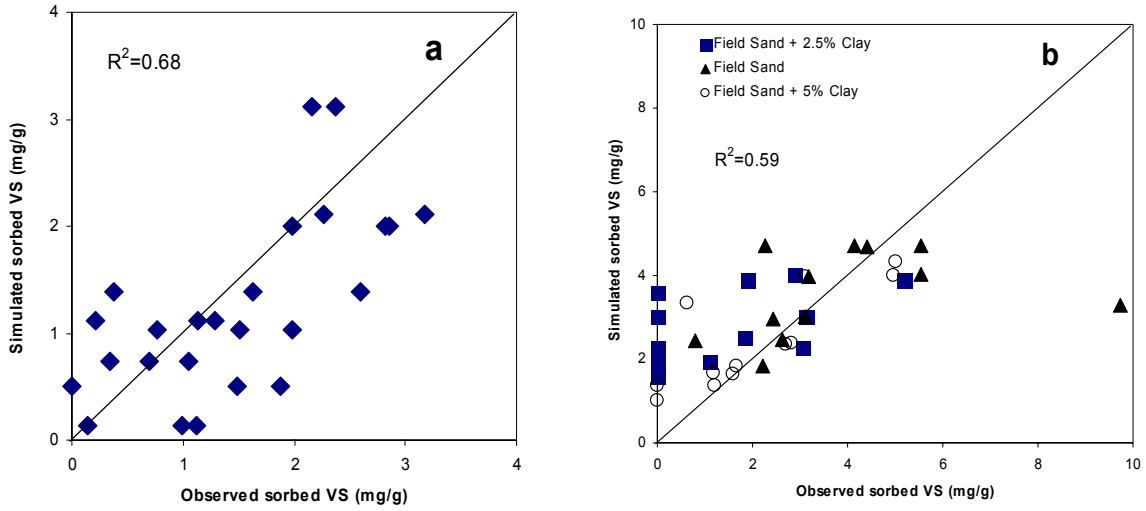

Figure 11 Comparison of simulated and observed sediment volatile solids concentration for homogeneous injection test (a) and heterogeneous injection test (b).

5. Summary and Conclusions

Emulsified edible oils can provide a low-cost, slow-release source of biodegradable organic carbon to support anaerobic bioremediation processes. However to be effective in the field, we must be able to effectively distribute the oil out away from the injection points without excessive permeability loss. Large-scale 3-D sandbox experiments were conducted for both homogeneous and heterogeneous conditions to evaluate the transport and distribution of emulsified edible oils under controlled laboratory conditions. Results from this work showed that injection of a fine oil-in-water emulsion (~ 0.1 PV for homogeneous, ~ 0.5 PV for heterogeneous) followed by chase water (~ 1.5 PV for homogeneous, ~ 5.5 PV for heterogeneous) resulted in excellent oil distribution throughout fine clayey sand with no significant reduction in hydraulic conductivity and no upward movement of the oil due to buoyancy effects. Data from both of these tests were used in the development and validation

of a 3-D numerical model of emulsion transport. All model parameters, with the exception of the mass transfer rate, were measured independently. Simulations results for both the homogeneous and heterogeneous injection tests were in close agreement with observed values. These results demonstrate that the transport and distribution of emulsified oil can be simulated using the numerical model RT3D with sorption represented by a mass-transfer limited, Langmuir isotherm. Additional research is needed to develop methods for independently estimating mass transfer rates that are representative of larger scale conditions.

Acknowledgement

The research presented in this manuscript was supported in part by Strategic Environmental Research and Development Program (SERDP) under project CU-1205.

References

ARCADIS Geraghty & Miller, Inc. (ARCADIS)., 2002. Final: Technical protocol for using soluble carbohydrates to enhance reductive dechlorination of chlorinated aliphatic hydrocarbons. Prepared for the Air Force Center for Environmental Excellence, San Antonio, Texas and the Environmental Security Technology Certification Program, Arlington, Virginia. December 19, 2002.

ASTM (American Society for Testing and Materials)., 2000. Designation: D 2434-68, Standard test method for permeability of granular soils (constant head), West Conshohocken, PA.

Borden, R. C., Coulibaly, K. M., Long, C. M., Harvin A. S., 2001. Development of permeable reactive barriers (PRBs) using edible oils, Annual Report to the Strategic Environmental Research and Development Program.

Brigham Young University, Environmental Modeling Laboratory, 1999. The Department of Defence Groundwater Modeling System, GMS v3.1.

Clement, T. P., 1997. RT3D – A modular computer code for simulating reactive multi-species transport in 3-Dimensional groundwater aquifers. Battelle Pacific Northwest National Laboratory Research Report, draft version, PNNL-SA-28967.

Coulibaly, K. M., Borden, R. C., 2003. Distribution of edible oil emulsions and permeability loss in sandy sediments, In Situ and On-Situ Bioremediation: The Seventh Internat. Sym., Orlando, FL (accepted for publication).

Coulibaly, K. M., Long, C. M., Lindow, N. L., Borden, R. C., 2003. Transport of edible oil emulsions in aquifer sands: experimental and simulation results, submitted for review.

Ellis, D.E., Lutz, E.J., Odom, J.M., Buchanan, R.J., Bartlett, C.L., Lee, M.D., Harkness, M.R., Deweerd, K.A., 2000. Bioaugmentation for accelerated in situ anaerobic bioremediation. Env. Sci. Tech. 34, 2254-2260.

Enfield, C. G., Bengtsson, G., Lindqvist, R., 1989. Influence of macromolecules on chemical transport, Environ. Sci. Technol. 23, 1278-1286.

Grindrod, P., 1993. The impact of colloids on the migration and dispersal of radionuclides within fractured rock. In: Chemistry and migration of actinides and fission products. Journal of Contam. Hydrol. 13, 167-182.

Grindrod, P., Edwards, M. S., Higgo, J. J. W., Williams, G. M., 1996. Analysis of colloid and tracer breakthrough curves. Journal of Contam. Hydrol. 21, 243-253.

Harkness, M. R., 2000. Economic considerations in enhanced anaerobic biodegradation: Bioremediation and phytoremediation of chlorinated and recalcitrant compounds. 2nd Internat. Conf. Remediation of Chlorinated and Recalcitrant Compounds. Monterey, California, May 22-25, 2000.

Harkness, M. R., R. Farnum, B. Weesner, D. Foti, W. Wilke, D. Smith, 2003. The case for chitin, In Situ and On-Situ Bioremediation: The Seventh Internat. Sym., Orlando, FL (accepted for publication).

Higgo, J. J. W., Williams, G. M., Harrison, I., Warwick, P., Gardiner, M. P., Longworth, G. 1993. Colloid transport in a glacial sand aquifer. Laboratory and field studies. Colloids and Surfaces A. 73, 179-200.

Hunter, W. J., 2001. Use of vegetable oil in a pilot-scale denitrifying barrier. J. Cont. Hydro. 53, 119-131.

Hunter, W. J., 2002. Bioremediation of chlorate or perchlorate contaminated water using permeable barriers containing vegetable oil. Current Microbiol., 45, 287-292.

Interstate Technology and Regulatory Council (ITRC) In Situ Bioremediation Team. 2002. Technical/Regulatory Guidelines: A systematic approach to in situ bioremediation in groundwater including decision trees on in situ bioremediation for nitrates, carbon tetrachloride, and perchlorate. August.

Koenigsberg, S. S., 2000. Accelerated bioremediation of chlorinated compounds in groundwater. Selected Battelle Couference Papers. 1999-2000. Regenesis Bioremediation Products, San Clemente, CA.

Konikow, L. F., August, L. L., Voss, C. I., 2001. Effect of clay dispersion on aquifer storage and recovery in costal aquifers. Transport in porous media 43, 45-64.

Kretzschmar, R., Robarge, W. P., Amoozegar, A., 1995. Influence of natural organic matter on colloid transport through saprolite. Water Resources Research 31 (3), 435-445.

Kretzschmar R., Sticher, H., 1998. Colloid transport in natural porous media: Influence of surface chemistry and flow velocity. Phys. Chem. Earth.23 (2), 133-139.

Lee, D.M., Lieberman T.M., Borden R.C., Beckwith W., Crotwell T. and Haas P.E., 2001. Effective distribution of edible oils – results from five field applications. – In: Wickramanayake, G.B., Gavaskar, A.R., Alleman, B.C., Magar, V.S. (Eds.), Proc. In Situ and On-Site Bioremediation: The Sixth Internal. Sym., San Diego, CA, Battelle Press, Columbus, OH.

Major, D.W., McMaster, M.L., Cox, E.E., Edwards, E.A., Dworatzek, S.M., Hendrickson, E.R., Starr, M.G., Payne, J.A., Buonamici, L.W., 2002. Field demonstration of successful bioaugmentation to achieve dechlorination of tetrachloroethene to ethene. Environ. Sci. Technol. 36, 5106-5116.

Martin, J.P., Sorenson, K.S., Peterson, L.N., 2001. Favoring efficient in situ dechlorination through amendment injection strategy. In: G. B. Wickramanayake, G.B., Gavaskar, A.R., Alleman, B.C., Magar, V.S. (Eds.): Proc. In Situ and On-Site Bioremediation: The Sixth Internal. Sym., San Diego, CA, pp. 265-272.

Martin, J. P., Sorenson, Jr. K. S., Peterson, L. N., Brennan, R. A., Werth, C. J., Sanford, R. A., Bures, G. H., Taylor, C. J., 2002. Enhanced CAH dechlorination in a low permeability variably-saturated medium, In: A.R. Gavaskar and A.S.C. Chen (Eds.), Remediation of Chlorinated and Recalcitrant Compounds, Battelle Press.

McAuliffe, C. D., 1973. Oil-in-water emulsions and their flow properties in porous media. Journal of Petroleum Technology, 727-733.

McDonald, J. M., Harbaugh, A. W., 1988. A modular three-dimensional finite-difference groundwater flow model, Techniques of water resources investigations of the U.S. Geological Survey Book 6, 586.

Morse, J. J., Alleman, B. C., Gossett, J. M., Zinder, S. H., Fennell, D. E., Sewell, G. W., Vogel, C. M. 1998. Draft technical protocol: A treatability test for evaluating the potential applicability of the reductive anaerobic biological in situ treatment technology (RABITT) to remediate chloroethenes. ESTCP, February 23, 1998.

Nyer, E. K., 1985. Groundwater treatment technology. Van Nostrand Reinhold, New York,

Ryan, J. N., Gschwend, P. M., 1994. Effect of solution chemistry on clay colloid release from an iron oxide-coated aquifer sand. Environ. Sci. Technol. 28, 1717-1726.

Soo H., Radke, C. J., 1986. A filtration model for the flow of dilute stable emulsions in porous media – I. Theory. Chemical Engr. Sci. 41, 263-272.

Thomas, J. M., Ward, C. H., 1989. In situ biorestoration of organic contaminants in the subsurface. Environ. Sci. Tech., 23 (7), 760-766

Wiedemeier, T. H., Henry, B. M., Haas, P. E., 2001. Technical protocol for enhanced reductive dechlorination via vegetable oil injection. Proceedings of the Sixth In Situ and On-Site Bioremediation Symposium. Battelle Press, Columbus, OH.

Wu, M., 1999. A pilot study using HRC^{TM} to enhance bioremediation of CAHs. Engineered approaches for In Situ Bioremediation of Chlorinated Solvent Contamination, Battelle Press, Columbus, Ohio, pp 177-180.

Zenker, M.J., Borden, R.C., Barlaz, M.A., Lieberman, M.T., Lee M. D., 2000. Insoluble substrates for reductive dehalogenation in permeable reactive barriers. In: Wickramanayake, G.B., Gavaskar, A.R., Alleman, B.C., Magar, V.S. (Eds) Bioremediation and Phytoremediation of Chlorinated and Recalcitrant Compounds, Battelle Press. pp. 47-53.

Zheng, C. 1990. MT3D - A modular three-dimensional transport model for simulation of advection, dispersion and chemical reactions of contaminants in groundwater system prepared for the U.S. Environmental Protection Agency.

Appendix A – Homogeneous Test

Appendix A1 – Emulsions - 1.2 μm median of droplet diameter by using a standard high-speed lab blender (Waring Commercial Blender).

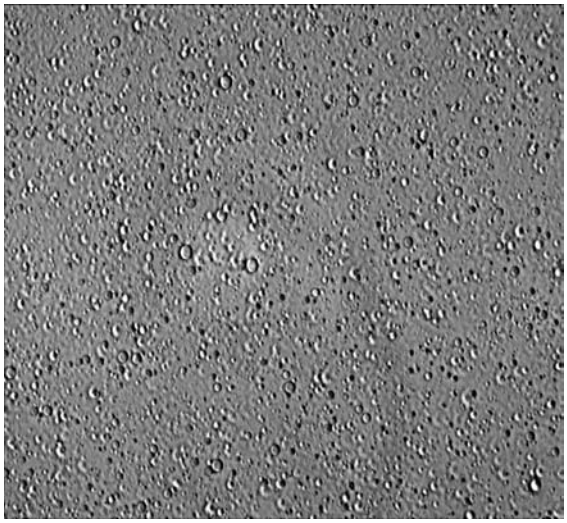

Appendix A2 – Homogeneous Sandbox Construction

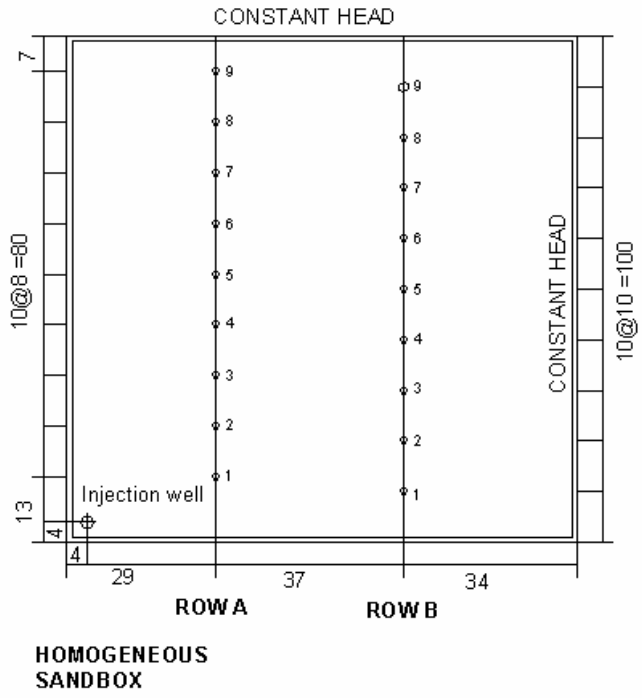

Table A1 Sample/Monitor Tube Locations for Homogeneous Sandbox

Layer 1 intakes are 75 cm from top of tank						
Sample Port No.	A1	A4	A7	B1	B4	B7
Radial Distance from Injection Well (cm)	26.6	46.3	73.4	62.3	71.7	90.5
Layer 2 intakes are 50 cm from top of tank						
Sample Port No.	A2	A5	A8	B2	B5	B8
Radial Distance from Injection Well (cm)	31.4	55.0	82.9	64.0	77.2	98.1
Layer 3 intakes are 25 cm from top of tank						
Sample Port No.	A3	A6	A9	B3	B6	B9
Radial Distance from Injection Well (cm)	38.3	64.1	92.4	67.2	83.5	106.0

Appendix A3 – Hydraulic and Tracer Test Results

Prior to the start of emulsion injection, the variation in head with radial distance from injection well is shown in Figure A1. As expected, head decreases with radial distance. Head difference between the top, middle and bottom layers is not significant with suggesting reasonably uniform flow through tank. Calculated head distribution using Theim equation is shown with the variation in head.

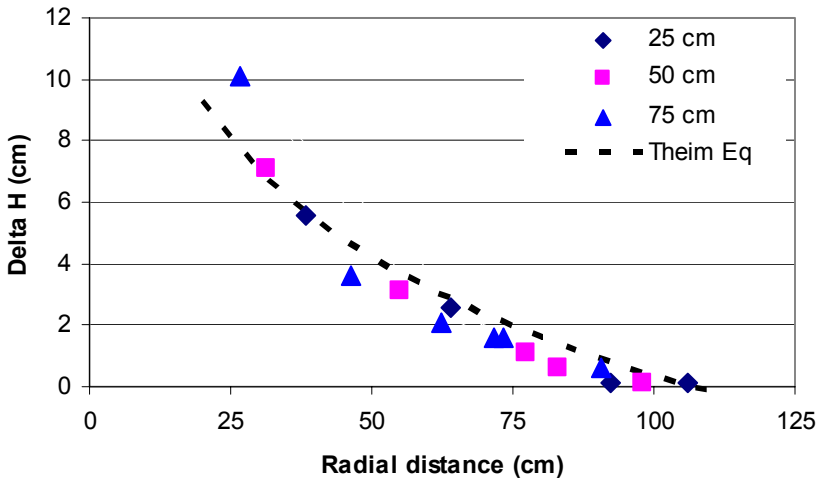

Fig. A1 Variation in head with radial distance from injection point prior to emulsion injection.

Appendix A4 – Emulsion Injection Test Results

Figure A2 shows the variation in fluid injection rate versus time during the emulsion injection test. Emulsion and chase water were injected over a 97 hour period with time = 0 as the start of emulsion injection. By recording the time required to inject 30 L of fluid (emulsion or water) flow rate was measured. Throughout the emulsion injection test, the head in the injection well was maintained 18 cm head above the level in the constant head boundaries. Based on a 5-day non-reactive tracer test conducted prior to emulsion injection, the pre-injection flow rate was 0.13 m^3 /d. As McAuliffe (1973) reported, during the emulsion injection, there was only a small reduction in flow rate, presumably due to the somewhat higher viscosity of the emulsion (1.44 centipoises) and lower density (0.99 g/cm^3). Whereas flow rate was recovered to that of the pre-injection right after finishing the emulsion injection suggesting there was no significant permeability loss during the test. The piezometer reading over the course of the test indicates there is no measurable change in water levels (data not shown).

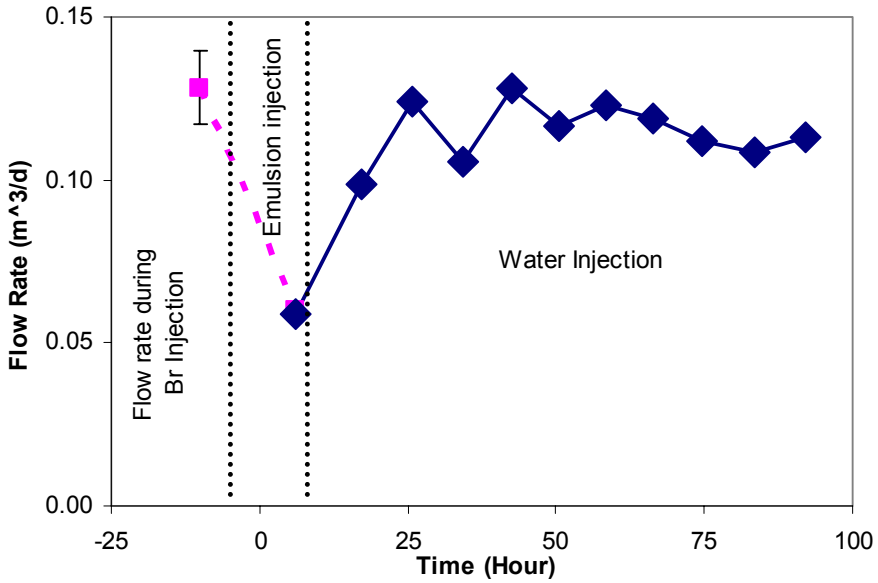

Fig. A2 Variation in injection flow rate with time during the homogenous injection test.

Appendix B – Heterogeneous Test

Appendix B1 – Emulsions - 0.7 μm median of droplet diameter by using a high pressure dairy homogenizer (Gaulins two stage 300 GCI at 1000 psi)

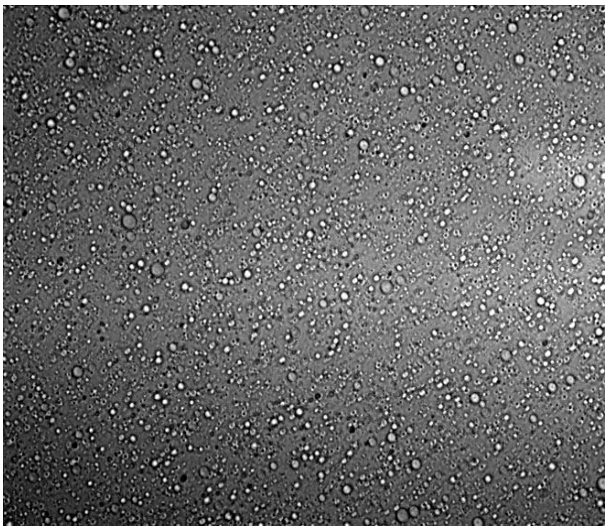

Appendix B2 – Heterogeneous Sandbox Construction

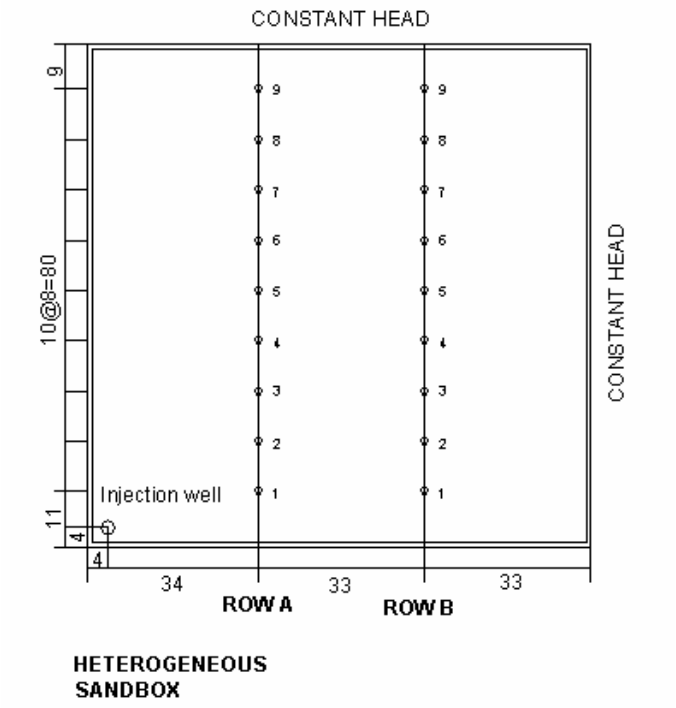

Table B1 Sample/Monitor Tube Locations for heterogeneous sandbox

Layer 1 (5% Clay sand layer) intakes are 90 cm from top of tank						
Sample Port No.	A1	A4	A7	B1	B4	B7
Radial Distance from Injection Well (cm)	35.7	53.3	78.7	67.9	78.5	97.6
Layer 2 (Field sand layer) intakes are 50 cm from top of tank						
Sample Port No.	A2	A5	A8	B2	B5	B8
Radial Distance from Injection Well (cm)	40.0	61.3	87.8	70.2	84.2	105.1
Layer 3 (2.5 % Clay sand) intakes are 20 cm from top of tank						
Sample Port No.	A3	A6	A9	B3	B6	B9
Radial Distance from Injection Well (cm)	46.0	69.8	97.1	73.8	90.6	113.0

Appendix B3 – Hydraulic and Tracer Test Results

Before the emulsion injection, tap water was passed through the heterogeneous sand box at a constant flow rate (q_t= 0.598 m^3/d) for several weeks to establish steady state conditions. Figure B1 shows the variation of head distribution with radial distance. There are slightly different heads between layer 1 (field sand + 2.5% clay) and layer 2 (field sand) except layer 3 (field sand + 5% clay). Hydraulic heads in Layer 1 and 2 are well matched and the measurement using ASTM d 2434 for permeability of granular soils (constant head) also indicates permeability of those two layers has no significant different (Data not shown). The dashed lines show the head calculated using the Theim equation.

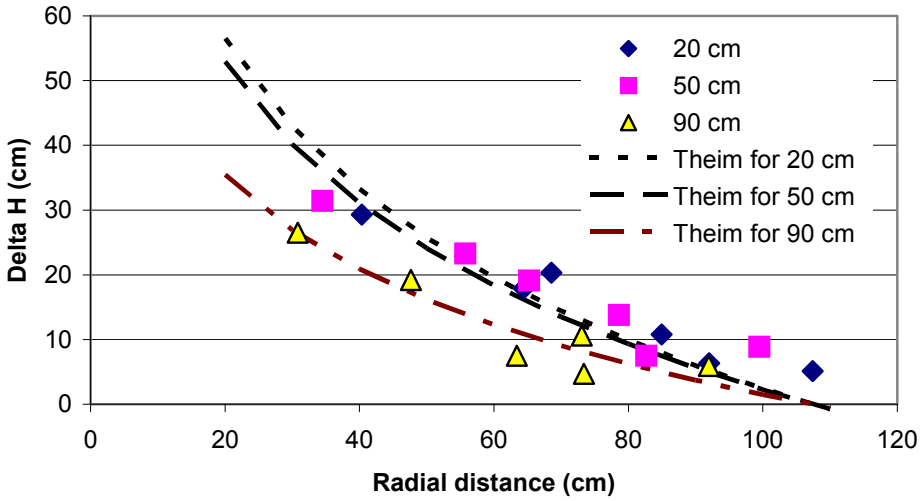

Fig. B1 Variation in head with radial distance from injection point prior to emulsion injection for heterogeneous sandbox.

Appendix B4 – Emulsion Injection Test Results

Figure B2 shows the variation in injection flowrate with time. Emulsion was injected from 0 to 10 hours followed by tap water injection for 70 hours or approximately 5.0 PV. The head difference between water supply reservoir and constant head reservoir was held constant at 58 cm which is higher than the 18 cm used during the homogeneous injection test. During emulsion injection, the flow rate dropped from 25 L/h (flow rate before emulsion injection) to 10~15 L/h and then the flow rate was recovered to the pre-injection flow rate. However, after 40 hours flow rate was gradually decreased to 8 L/h. We hypothesize that kaolinite added to the upper and lower layers (Field Sand + 2.5 % clay and Field sand + 5% clay) was mobilized by the surfactant used to form the emulsion, causing clogging of the non-woven geotextile that formed the constant head boundary. Clay mobilization by surfactants (Ryan et al., 1994) can also effective the aquifer permeability (Konikow et al., 2001)

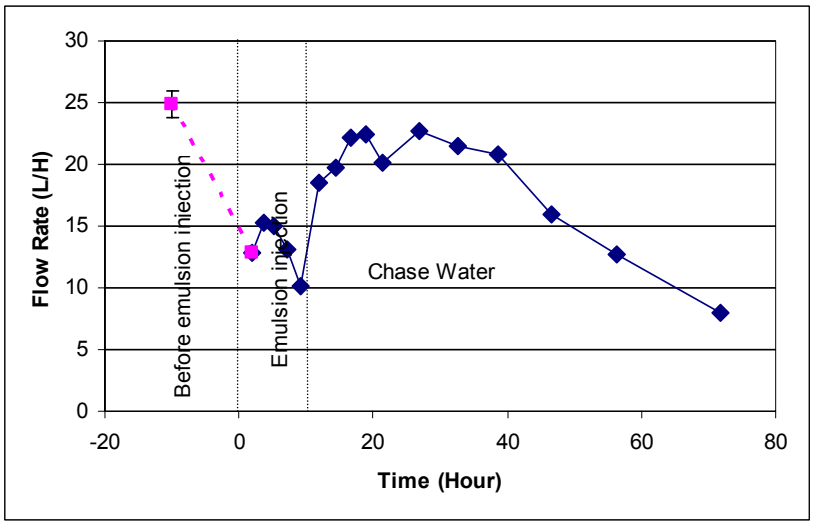

Fig. B2 Variation in injection flow rate with time during the emulsion injection for heterogeneous sandbox

Appendix C - Volatile Solid in Final Sediment

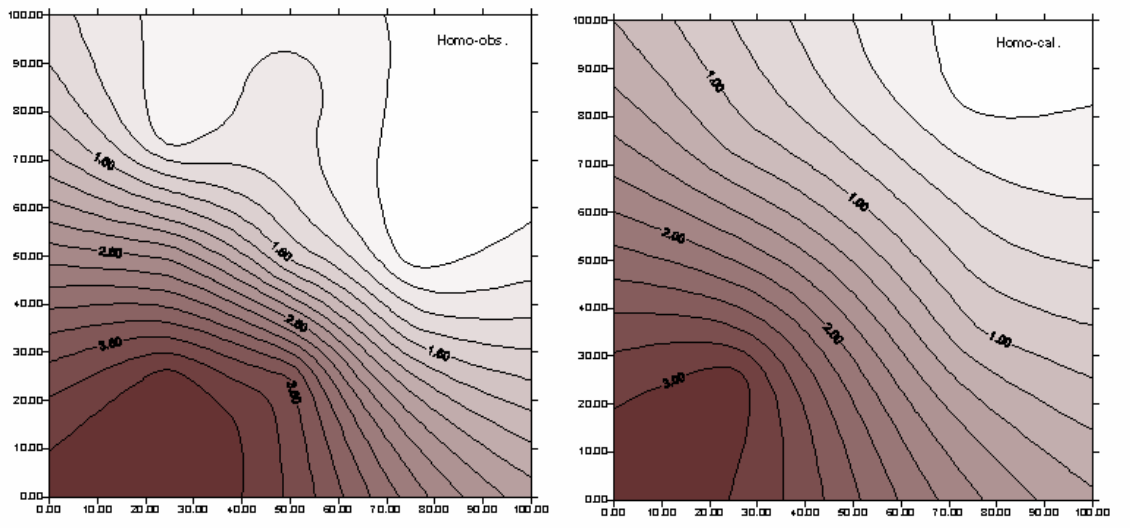

Fig. C1 Volatile solids in sediment from experimental results (left) and simulation result for homogenous sandbox (Surfer 3.1).

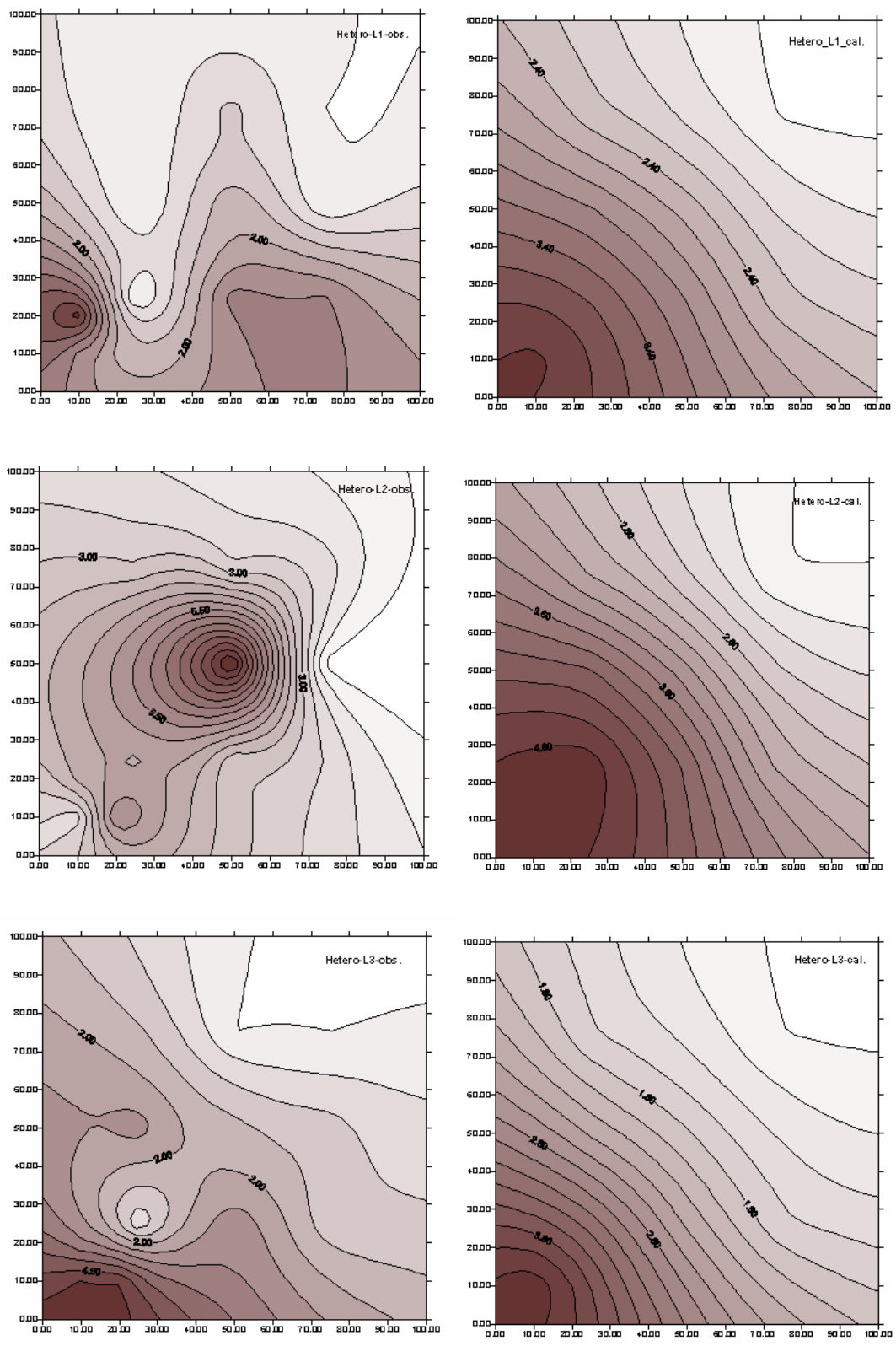

Fig. C2 Volatile solids in sediment from experimental results (left) and simulated result for heterogeneous sandbox (Surfer 3.1).